BIOCHEMISTRY
including biophysical chemistry & molecular biology

Article

pubs.acs.org/biochemistry

Thalidomide (5HPP-33) Suppresses Microtubule Dynamics and Depolymerizes the Microtubule Network by Binding at the Vinblastine Binding Site on Tubulin

Aijaz Rashid, Annapurna Kuppa, Ambarish Kunwar, and Dulal Panda*

Department of Biosciences and Bioengineering, Indian Institute of Technology Bombay, Mumbai 400076, India

Supporting Information

ABSTRACT: Thalidomides were initially thought to be broad-range drugs specifically for curing insomnia and relieving morning sickness in pregnant women. However, its use was discontinued because of a major drawback of causing teratogenicity. In this study, we found that a thalidomide derivative, 5-hydroxy-2-(2,6-diisopropylphenyl)-1*H*-isoindole-1,3-dione (5HPP-33), inhibited the proliferation of MCF-7 with a half-maximal inhibitory concentration of 4.5 ± 0.4 μM. 5HPP-33 depolymerized microtubules and inhibited the reassembly of cold-depolymerized microtubules in MCF-7 cells. Using time-lapse imaging, the effect of 5HPP-33 on the dynamics of individual microtubules in live MCF-7 cells was analyzed. 5HPP-33 (5 μM) decreased the rates of growth and shortening excursions by 34 and 33%, respectively, and increased the time microtubules spent in the pause state by 92% as compared to that of the vehicle-treated MCF-7 cells. 5HPP-33 (5 μM) reduced the dynamicity of microtubules by 62% compared to the control. 5HPP-33 treatment reduced the distance between the two poles of a bipolar spindle, induced multipolarity in some of the treated cells, and blocked cells at mitosis. *In vitro*, 5HPP-33 bound to tubulin with a weak affinity. Vinblastine inhibited the binding of 5HPP-33 to tubulin, and 5HPP-33 inhibited the binding of BODIPY FL-vinblastine to tubulin. Further, a molecular docking analysis suggested that 5HPP-33 shares its binding site on tubulin with vinblastine. The results provided significant insight into the antimitotic mechanism of action of 5HPP-33 and also suggest a possible mechanism for the teratogenicity of thalidomides.

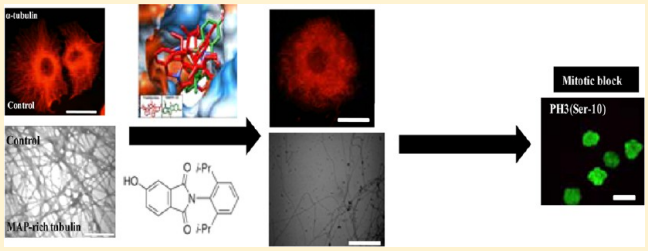

Thalidomide was discovered in 1950s as a broad-range drug.[1] It was initially used to cure insomnia and was also found to be helpful in relieving morning sickness in pregnant women. The drug was withdrawn from the market because of its teratogenic effects.[2] However, the drug has been approved by the Food and Drug Administration for the treatment of Hansen's disease and multiple myeloma.[1] Thalidomide may have potential uses in the treatment of several other diseases.[3] Thalidomide was also in clinical trials in hormone-dependent prostate cancer (ClinicalTrials.gov Identifier NCT00004635), HIV ulcers and viremia (ClinicalTrials.gov Identifiers NCT00000790 and NCT00001524), HIV-related Kaposi's sarcoma (ClinicalTrials.gov Identifier NCT00019123), Sjogren's syndrome (ClinicalTrials.gov Identifier NCT00001599), and host-versus-graft disease (ClinicalTrials.gov Identifiers NCT00003894 and NCT00075023). Thalidomide and its derivatives act as a template for the development of several biologically active compounds.[1] Several thalidomide analogues have been developed over the years, which are categorized according to their biological effects,[1] for example, TNF-α production regulators,[4] thymidine phosphorylase inhibitors,[5] cyclooxygenase inhibitors,[6] histone deacetylase inhibitors,[7] anti-angiogenic agents,[8] cell differentiation inducers,[9] and tubulin inhibitors.[10,11]

Thalidomide is a metabolically unstable compound.[12] The side effects of thalidomide immensely depend on its metabolism,[12,13] and therefore, thalidomide metabolism was studied in different organisms.[14] The identification of active metabolites of thalidomide not only will enhance the drug activity by the selective usage of those metabolites for different diseases but also might reduce the side effects caused by an overload of accessory metabolites. The metabolism of thalidomide produces two inhibitors of tubulin polymerization, namely, 5-hydroxythalidomide and *N*-hydroxythalidomide.[1]

Several proposals were invoked to explain the causative reasons for the thalidomide-induced teratogenicity.[15] The intercalation of thalidomide with the G-C box promoter of some important genes such as Fgf2 and insulin-like growth factor-1 (Igf1), which are vital for limb growth, can be the cause for the thalidomide-induced teratogenicity.[16] Thalidomide generates reactive oxygen species, which can oxidize and mutate DNA, and thereby may cause teratogenicity.[17] Recently, it has been proposed that the direct binding of thalidomide to CRBN inhibits its E3 ubiquitin ligase activity, leading to the accumulation of its substrates, which produces developmental

Received: November 19, 2014
Revised: February 25, 2015
Published: March 6, 2015

DOI: 10.1021/bi501429j
Biochemistry 2015, 54, 2149–2159

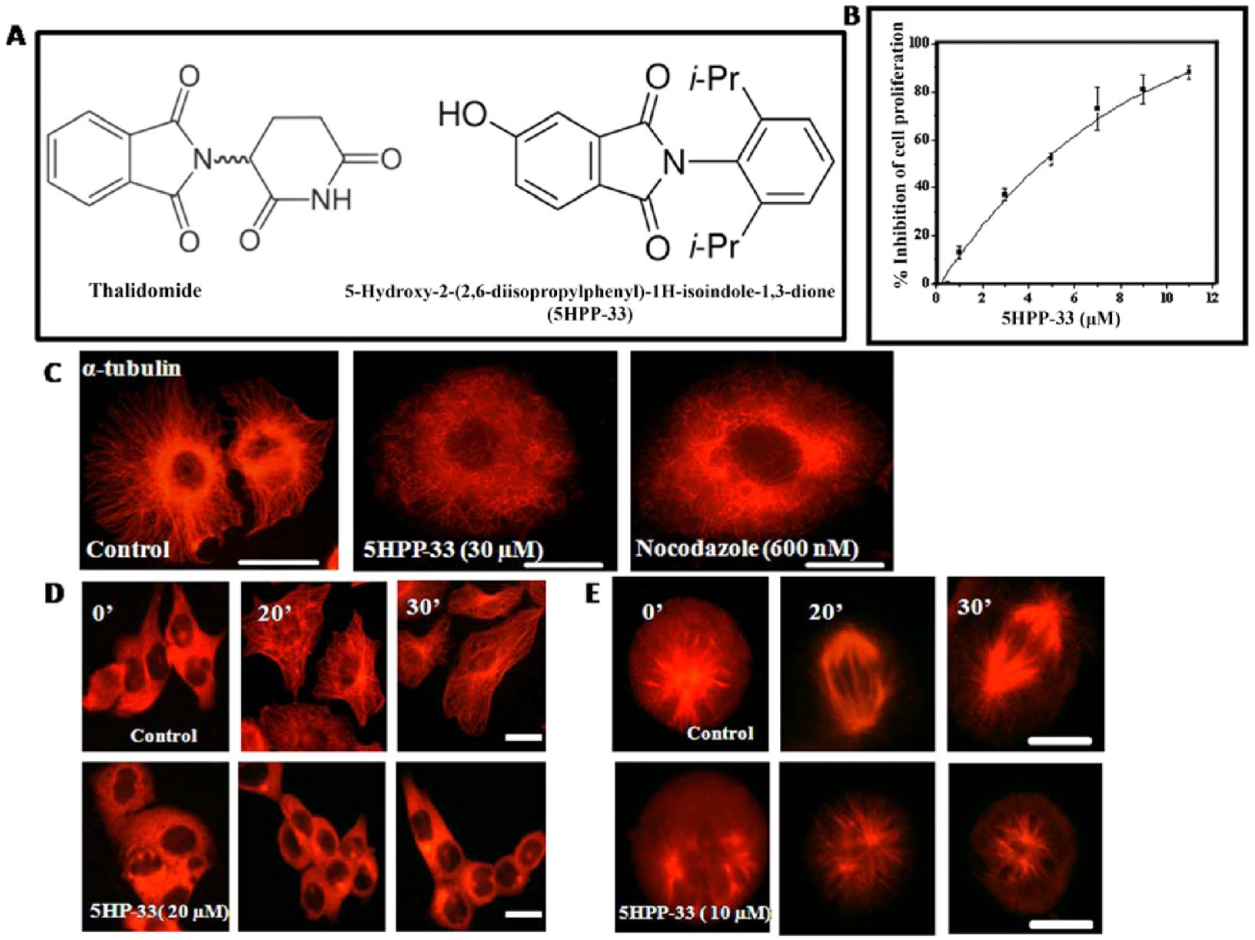

Figure 1. 5HPP-33 inhibited the proliferation of MCF-7 cells and perturbed the assembly of microtubules in these cells. (A) Chemical structures of thalidomide and 5HPP-33 are shown. (B) 5HPP-33 inhibited the proliferation of MCF-7 cells in culture. (C) A brief exposure of 5HPP-33 depolymerized microtubules in MCF-7 cells. Cells were incubated with 30 μM 5HPP-33 for 3.5 h. Nocodazole (600 nM) was used as a positive control for depolymerization. (D) 5HPP-33 (20 μM) prevented the reassembly of microtubules in MCF-7 cells after cold-induced depolymerization. (E) 5HPP-33 (10 μM) inhibited the reassembly of cold-depolymerized spindle microtubules. The scale bar is 10 μm.

defects such as limb deformities.[2] D'Amato and co-workers found a positive correlation between the anti-angiogenic activity of thalidomides and its teratogenic effects and proposed that the anti-angiogenic activity of thalidomides as the cause for its teratogenic effect.[18]

Inhibitors of microtubule dynamics are found to have potent anti-angiogenic activity,[19,20] and the assembly dynamics of microtubules play an essential role in cell division.[20,21] On the basis of the structure of a tubulin targeting metabolite of thalidomide (5-hydroxythalidomide), 5-hydroxy-2-(2,6-diisopropylphenyl)-1*H*-isoindole-1,3-dione (5HPP-33) was developed (Figure 1A).[1,22] 5HPP-33 showed cytotoxicity in several cancer cell lines.[1] In the *in vitro* system, 5HPP-33 was reported to be an inhibitor of tubulin polymerization and also depolymerized microtubules in cultured cells.[23] In addition, 5HPP-33 and a trifluorinated analogue of 5HPP-33 (5HFPP-33) did not influence either cold or $CaCl_2$-induced depolymerization of microtubules but prevented re-formation of microtubules after cold-induced depolymerization.[22,23] It caused G2/M block[24] of cell cycle progression followed by caspase-3-dependent apoptosis.[22,24] However, another study suggested that 5HPP-33 showed paclitaxel-like polymerization enhancing effects on microtubules.[25] Therefore, the effects of 5HPP-33 on microtubules are not clear. Interestingly, 5HPP-33 did not show any competition with radiolabeled colchicine or vinblastine for tubulin binding, indicating that it may bind to tubulin at a site that is different from these sites.[23]

In this study, 5HPP-33 was found to depolymerize microtubules in MCF-7 cells and to inhibit the assembly of both MAP-rich tubulin and purified tubulin *in vitro*. Further, the compound suppressed the dynamic instability of microtubules in live MCF-7 cells. 5HPP-33 bound to tubulin with a weak affinity. Both experimental and theoretical data obtained in this study suggested that 5HPP-33 shares its binding site on tubulin with vinblastine. Inhibitors of microtubule dynamics have been found to retard cell migration.[26] Thalidomide was found to inhibit cell migration and slow wound healing in cultured cells.[27] An impairment of cell migration can produce severe complications during the developmental stages of an embryo.[28] Thus, the data indicated that thalidomide-mediated teratogenicity can be partially due to the alteration of microtubule dynamics.

EXPERIMENTAL PROCEDURES

Hoechst 33258 and the rabbit anti-phosphohistone 3 (PH3) antibody were purchased from Santa Cruz Biotechnology (Santa Cruz, CA). Monoclonal mouse anti-α-tubulin IgG, mouse antiacetylated tubulin IgG, rabbit polyclonal anti-γ-tubulin, FITC-labeled anti-rabbit IgG conjugate, and bovine

DOI: 10.1021/bi501429j
Biochemistry 2015, 54, 2149−2159

serum albumin (BSA) were purchased from Sigma. Anti-mouse IgG-Alexa 568 was purchased from Molecular Probes. Other chemicals were purchased from Sigma (St. Louis, MO) and Himedia (Mumbai, India).

Cell Culture. MCF-7 and MDA-MB-231 cells were procured from the National Centre for Cell Science (Pune, India). MCF-7 cells were grown in MEM (Eagle's minimal essential medium) (Himedia). MEM contains 10% fetal bovine serum, 2.2 g/L sodium bicarbonate, and a 1% antibiotic/antimycotic solution composed of streptomycin, amphotericin B, and penicillin. Cells were grown at 37 °C in a humidified atmosphere of 5% carbon dioxide. Cells were maintained in a 25 mL cell culture flask (Nunc) at 37 °C in an incubator.

Cell Proliferation Assay. MCF-7 cells (1×10^5 cells/mL) were seeded in a polylysine-coated 96-well plate for 24 h. Cells were incubated with either vehicle (control) or different concentrations of 5HPP-33 for 48 h. The effect of 5HPP-33 on MCF-7 cell proliferation was determined by a Sulforhodamine B (SRB) assay.[29] The experiment was performed three times.

Microtubule Organization and Network in an MCF-7 Cell Line. MCF-7 (0.5×10^5 cells/mL) cells were seeded on a polylysine-coated glass coverslips in 24-well plates for 24 h and then incubated with either vehicle (control) or 5 and 10 μM 5HPP-33 for 24 h. Subsequently, cells were spun at 2500 rpm and 25 °C for 10 min in a 24-well plate to collect the loosely bound mitotic cells, fixed with 3.7% formaldehyde, and immunostained using an antibody against α-tubulin, acetylated tubulin (primary, 1:300; secondary, 1:300). The experiment was performed three times. For acetylated microtubule staining, cells were treated with 2 and 4 μM 5HPP-33 and stained. DNA was stained with Hoechst.[30] γ-Tubulin staining was performed using an antibody against γ-tubulin (primary, 1:2000; secondary, 1:800). Phosphohistone H3 staining[30] was performed using an antibody against phosphohistone (primary, 1:300; secondary, 1:300).

Effects of 5HPP-33 on the Reassembly of Cold-Depolymerized Microtubules in MCF-7 Cells. MCF-7 cells were grown for 24 h on glass coverslips in 24-well plates. Then, the medium was replaced with fresh medium and 5HPP-33 at a concentration of 20 μM. The plates were kept on ice for 45 min to depolymerize the microtubule network. Then, the cells were incubated at 37 °C for different time intervals (0, 20, and 30 min) in an incubator and fixed using 3.7% formaldehyde in PBS at 37 °C.[28] In a separate experiment, MCF-7 cells were blocked in mitosis by nocodazole (300 nM) treatment to enrich mitotic cell population. The MCF-7 cells were extensively washed to remove nocodazole, and then the cells were incubated on ice with fresh medium for 30 min. The reassembly of the mitotic spindle was observed at different time intervals in the presence and absence of 10 μM 5HPP-33 at 37 °C. Microtubules were stained as described previously.[31] The experiment was performed three times.

Measurements of Microtubule Dynamics in MCF-7 Cells. Transfection of the EGFP-α-tubulin plasmid in MCF-7 cells was done using lipofectamine-2000 following the manufacturer's protocol as described previously.[32] The transfected cells were seeded on the coverslips for 24 h and then treated with 5HPP-33 for 3 h. The dynamics of microtubules were monitored by time-lapse imaging of live MCF-7 cells expressing EGFP-tubulin using confocal microscopy. The cells were observed in the controlled temperature regulation under a 60× oil immersion objective by using a laser scanning confocal microscope (FluoView 500 Olympus, Tokyo, Japan). Fifty images of each cell were taken at 4 s interval, and the plus ends of microtubules were tracked using ImageJ. The dynamic instability parameters of microtubules were determined as described previously.[26,31−33] The individual microtubule length over time was plotted to obtain the life history track of microtubules. The convention followed to assign growth and shortening was an increase or decrease in length of ≥0.5 μm as a growth or a shortening phase, while a change of ≤0.5 μm in length was considered a pause state. The switching of a microtubule from either a growth or a pause state to a shortening state is called as catastrophe, while a transition from a shortening state to a pause or a growth state is called as rescue.[34] The catastrophic events were divided by the total time a microtubule spends in the growth or pause state to obtain the time-based catastrophic frequency. The rescue events were divided by the total time a microtubule spends in the shortening state to obtain the time-based rescue frequency, while the rescue events when divided by the total shortening length give the length-based rescue frequency. The dynamicity of individual microtubules was calculated by dividing the total length (growth and shortening length) by the life span of microtubules. The microtubules that were visible in all the frames were selected; 25 such microtubules for each sample were chosen, and different parameters of microtubule dynamics were calculated. The statistical significance was determined by one-way analysis of variance (ANOVA) using Origin7.5.

Tubulin Isolation. Tubulin was isolated from goat brain by two cycles of an assembly−disassembly process in the presence of 1 M glutamate and 10% (v/v) DMSO.[35,36] Binding experiments were performed using tubulin isolated by this method. The protein concentration was estimated by the Bradford method using bovine serum albumin as a standard.[37] The protein was stored at −80 °C for further use. MAP-rich tubulin was isolated by two cycles of assembly and disassembly in the presence of 4 M glycerol.[38] Tubulin was purified by passing MAP-rich tubulin through a phosphocellulose column.

Effects of 5HPP-33 on the Assembly Kinetics of MAP-Rich Tubulin and Phosphocellulose-Purified Tubulin *in Vitro*. MAP-rich tubulin (1 mg/mL) in 25 mM Pipes (pH 6.8) containing 3 mM $MgCl_2$ and 1 mM EGTA was incubated without or with 2.5, 5, 10, and 20 μM 5HPP-33 for 30 min on ice. Then, 1 mM GTP was mixed with the reaction mixtures, and the assembly was monitored by measuring the optical density at 350 nm using a plate reader at 37 °C (SpectraMax M2 Molecular Devices).

In addition, tubulin (13 μM) was incubated without or with different concentrations (5−30 μM) of 5HPP-33 in 25 mM Pipes (pH 6.8), 3 mM $MgCl_2$, 1 M glutamate, and 1 mM EGTA for 30 min at 4 °C. Then, 1 mM GTP was added to the reaction mixture, and the assembly kinetics of tubulin was followed using a plate reader at 37 °C. In a separate experiment, tubulin (13 μM) was incubated without or with different concentrations (10−30 μM) of 5HPP-33 in 25 mM Pipes buffer (pH 6.8) containing 3 mM $MgCl_2$, 1 mM EGTA, and 8% DMSO for 30 min at 4 °C. Then, 1 mM GTP was added to the reaction mixtures, and the assembly kinetics was monitored at 350 nm for 30 min at 37 °C.

Electron Microscopy. MAP-rich tubulin (1 mg/mL) polymerized in the presence and absence of different concentrations of 5HPP-33. Pure tubulin (10 μM) was polymerized in the presence of 1 M glutamate. Samples were fixed with 1% glutaryaldehyde and diluted 5-fold in PEM buffer. Electron microscope grids were immersed in sample drops, air-

DOI: 10.1021/bi501429j
Biochemistry 2015, 54, 2149−2159

dried, and fixed with 2% uranyl acetate. The samples were observed under a transmission electron microscope (FEI Tecnai-G^{2}12, Philips).

Measurement of the Dissociation Constant (K_d) Using Tryptophan Fluorescence of Tubulin and the 5HPP-33−Tubulin Complex. Tubulin (2 μM) in 25 mM Pipes buffer (pH 6.8) was incubated without or with different concentrations of 5HPP-33 at 25 °C for 20 min. After incubation for 20 min, tryptophan fluorescence was monitored using a 0.3 cm path length cuvette by exciting the reaction mixtures at 295 nm. The emission spectra (310−370 nm) were recorded. The fluorescence intensities were corrected for the inner filter effect.[31,39] The fluorescence changes were fit to the equation $\Delta F = \Delta F_{max} L/K_d + L$, where ΔF and ΔF_{max} represent the changes in fluorescence intensity of tubulin upon binding to 5HPP-33 and the maximal change in fluorescence intensity of tubulin when it is fully bound with 5HPP-33, respectively, and L is the concentration of 5HPP-33. ΔF_{max} was estimated using GraphPad Prism 5 (GraphPad Software, La Jolla, CA).

The fluorescence intensity of 5HPP-33 increased upon binding to tubulin. Tubulin (3 μM) was incubated without or with different concentrations (5−100 μM) of 5HPP-33 for 10 min at 25 °C. The fluorescence spectra (420−600 nm) were recorded using 350 nm as an excitation wavelength. The fluorescence spectrum of only 5HPP-33 was subtracted from the fluorescence spectra of 5HPP-33 in the presence of tubulin. The fluorescence intensity of 5HPP-33 was corrected for the inner filter effect as described previously.[31] The increase in the fluorescence intensity of 5HPP-33 upon binding to tubulin was used to determine the binding constant as described above.

Investigation of the 5HPP-33 Binding Site on Tubulin. Tubulin (3 μM) was incubated without or with different concentrations (20, 30, 50, and 60 μM) of vinblastine in pipes buffer (pH 6.8) for 30 min at 25 °C. 5HPP-33 (10 μM) was added to the reaction mixtures and incubated for an additional 10 min. The 5HPP-33−tubulin complex fluorescence was measured with excitation at 350 nm, and emission at 400−600 nm was monitored.

In a separate experiment, tubulin (2 μM) in 25 mM pipes buffer (pH 6.8) was incubated without or with different (10−50 μM) concentrations of 5HPP-33 for 30 min at 25 °C. BODIPY FL-vinblastine (2 μM) was added to the reaction mixtures, and samples were further incubated at 25 °C for an additional 20 min in the dark. Excitation of the tubulin−BODIPY FL-vinblastine complex was conducted at 490 nm, and the emission spectra were recorded in the range of 500−550 nm. Spectra were subtracted from only BODIPY FL-vinblastine.

In another experiment, tubulin (3 μM) was incubated without or with different concentrations of podophyllotoxin in pipes buffer (pH 6.8) for 30 min at 25 °C and then incubated with 5HPP-33 (10 μM) for an additional 20 min. The emission spectra (420−570 nm) were recorded using 350 nm as the excitation wavelength.

Identification of a Putative Binding Site of 5HPP-33 on Tubulin by Molecular Docking. The putative binding site of 5HPP-33 on tubulin was identified by Autodock 4.2.[40] The three-dimensional atomic coordinates of 5HPP-33 were generated using the PRODRG server.[41] Vinblastine and tubulin dimer, used for control docking, were acquired from Protein Data Bank entry 1Z2B.[42] Only those tubulin chains that interact with vinblastine, i.e., chain B (β) and chain C (α), were used as a template for all molecular docking studies. Initially, blind docking[43] was performed for both 5HPP-33 and vinblastine with tubulin dimer, by preparing grid boxes of 126 grid points in each of the X, Y, and Z directions, with 0.7 Å spacing. While enough space was provided for the movement of ligands, the tubulin dimer was treated as rigid in all the docking studies. Essential H atoms were also added to this tubulin dimer using UCSF Chimera.[44] All ligands and chains A, D, and E of PDB entry 1Z2B were removed from the crystal structure preceding docking. Both ligands, vinblastine and 5HPP-33, were tested by placing them at different random locations in the chosen grid box for each blind docking job performed. Blind docking involved 100 Lamarckian Genetic Algorithm (LGA) runs with 10 repetitions of ligand docking that resulted in 1000 output conformations for each case.[42] These results helped us to conclude that both 5HPP-33 and vinblastine are most likely to dock at the interface between β- and α-tubulin monomers.

Thus, only the $\beta-\alpha$ interface was considered for local docking of 5HPP-33 and vinblastine with tubulin dimer, with grid boxes of 126 grid points in each of the X, Y, and Z directions, with 0.35 Å spacing. All parameters in LGA were used as default, but g_eval was set to medium. Docking performed for vinblastine (control) and 5HPP-33 involved 100 LGA runs with 50 repetitions of flexible ligand docking, which yielded 5000 output conformations for each case.[45] These conformations were reclustered using a 4 Å all-atom root-mean-square deviation (rmsd) cutoff. The binding energies of all poses were calculated using the scoring functions employed by AutoDock 4.2.[40] In addition, comparison and analysis were performed for all clusters containing at least 20 conformations. These clusters were then compared on the basis of cluster size (number of conformations) and binding energy to determine the potent binding modes for both the ligands. UCSF Chimera was used to perform further analysis.[44]

RESULTS

5HPP-33 Depolymerized Microtubules and Inhibited Microtubule Assembly in MCF-7 Cells. 5HPP-33 (Figure 1A) inhibited the proliferation of MCF-7 cells in a concentration-dependent manner with a half-maximal inhibitory concentration of 4.5 ± 0.4 μM (Figure 1B). To ascertain the effects of 5HPP-33 on cellular microtubules, MCF-7 cells were incubated with 30 μM 5HPP-33 for 3.5 h. Similar to the effect of 600 nM nocodazole, a short exposure of 5HPP-33 (30 μM) caused extensive depolymerization of microtubules in MCF-7 cells (Figure 1C). To further explore the effects of 5HPP-33 on microtubule growth, a microtubule reassembly experiment after cold-induced depolymerization was performed. Microtubules in vehicle-treated cells grew rapidly and established a proper microtubule network within 30 min, while 5HPP-33 treatment prevented microtubule formation, suggesting that the assembly of microtubules in 20 μM 5HPP-33-treated cells was much slower than that in the vehicle-treated cells (Figure 1D). Further, the treatment with 5HPP-33 also hampered the rebuilding of mitotic spindles, indicating that 5HPP-33 inhibited growth of spindle microtubules (Figure 1E).

5HPP-33 Treatment Depolymerized Microtubules, Caused Multipolar Spindle Formation, and Decreased the Interpolar Distance in the Bipolar Spindles. The effect of 5HPP-33 (5 and 10 μM) on microtubules was examined after treatment for 24 h. Similar to the effects of several microtubule inhibitors,[30,31,45] 5HPP-33 treatment was found to depolymerize both interphase and spindle microtubules in MCF-7 cells (Figure 2A,B). 5HPP-33 treatment

DOI: 10.1021/bi501429j
Biochemistry 2015, 54, 2149−2159

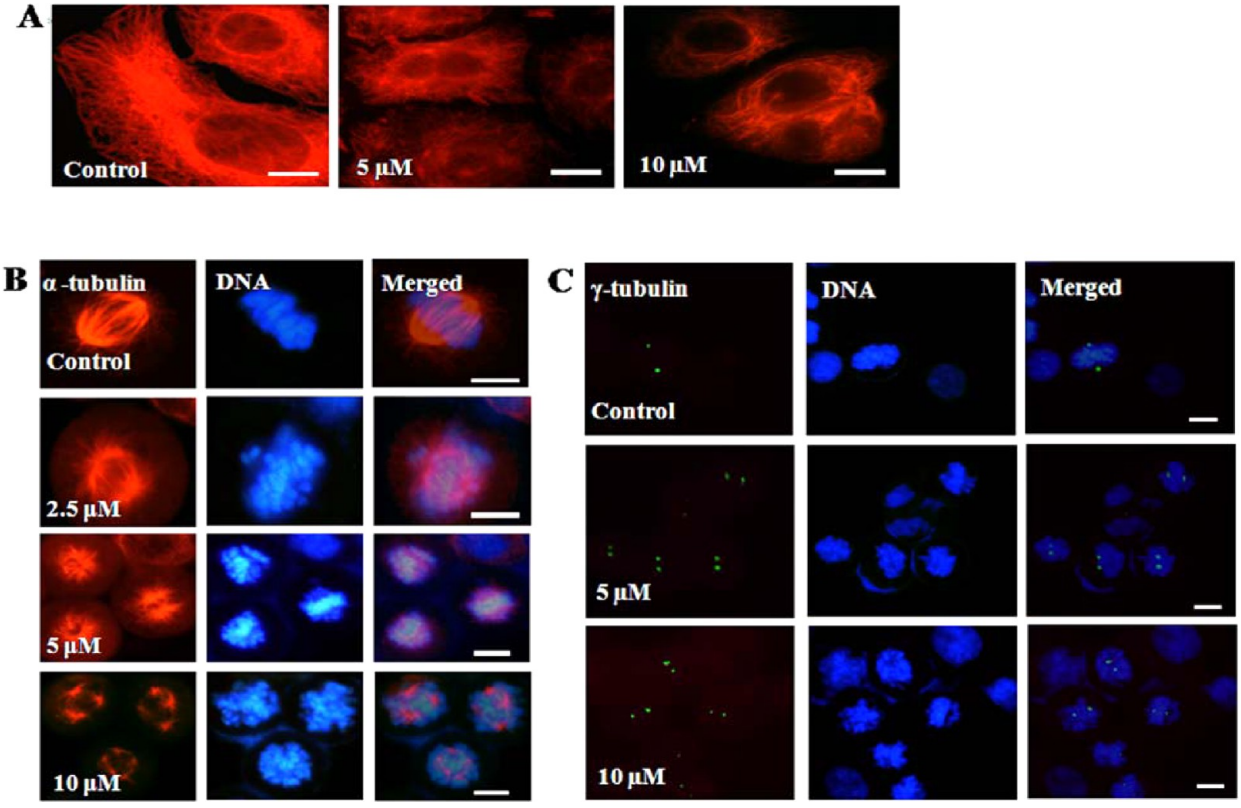

Figure 2. 5HPP-33 depolymerized the microtubule network in MCF-7 cells and caused multipolar spindle formation. (A and B) MCF-7 cells were incubated without or with 5 and 10 μM 5HPP-33 for 24 h. 5HPP-33 depolymerized both interphase (A) and spindle (B) microtubules. The mitotic spindles showed multipolarity in the presence of 5HPP-33 (B). (C) 5HPP-33 treatment reduced the distance between two poles of a bipolar spindle as shown by γ-tubulin staining (n = 20 under each condition). Scale bars are 10 μm.

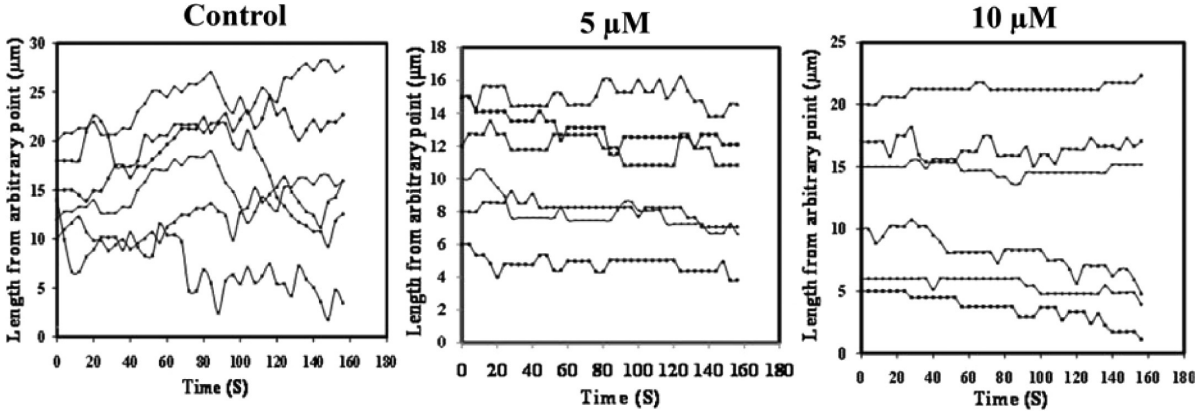

Figure 3. 5HPP-33 suppressed microtubule dynamics in live MCF-7 cells measured by time-lapse imaging. Life history traces depicting microtubule length change with time in vehicle-treated control MCF-7 cells and in the presence of 5 and 10 μM 5HPP-33 are shown. The initial length was chosen arbitrarily, and the change in length was demarked at each time point by tracking the plus end of the microtubules.

caused spindle abnormality in MCF-7 cells (Figure 2B). The alignment of chromosomes at the metaphase plate was compromised, and several lagging chromosomes were observed in the 5HPP-33-treated cells (Figure 2B). The compound also induced multipolar and monopolar mitotic spindle formation (Figure 2B). Further, the average distance between the two spindle poles was found to be 10.3 ± 1, 5.3 ± 1.3, and 4.8 ± 1.5 μm in the absence and presence of 5 and 10 μM 5HPP-33, respectively, suggesting that 5HPP-33 decreased the distance between the two poles of a bipolar spindle (Figure 2C). 5HPP-33 (10 and 20 μM) was also found to depolymerize microtubules in highly metastatic breast cancer cells (MDA-MB231) (Figure S1 of the Supporting Information).

In addition, 5HPP-33 treatment produced an increase in the level of acetylation of microtubules as compared to that of the vehicle-treated MCF-7 cells, indicating that the compound might suppress microtubule dynamics (Figure S2A of the Supporting Information). Histone H3 is a marker of mitotic cells as metaphase chromosomes are phosphorylated at the hydroxyl group of serine 10 during cell cycle progression.[46] 5HPP-33 treatment increased the number of phosphohistone positive cells (Figure S2B of the Supporting Information). For example, 3 ± 1, 22 ± 4, and 36 ± 7% of cells showed

DOI: 10.1021/bi501429j
Biochemistry 2015, 54, 2149−2159

phosphohistone positive staining in the absence and presence of 5 and 10 μM 5HPP-33, respectively, suggesting that 5HPP-33 blocked cell cycle progression at mitosis (Figure S2B of the Supporting Information). Phosphohistone positive cells further showed spatial disorganization of chromosomes in the treated cells as compared to the control cells.

5HPP-33 Treatment Caused Multinucleation in MCF-7 Cells. MCF-7 cells were incubated with either the vehicle or 5HPP-33 for 48 h. In vehicle-treated MCF-7 cells, only 2 ± 1% of cells were multinucleated while 50 ± 7 and 62 ± 9% of cells were multinucleated in the presence of 10 and 20 μM 5HPP-33, respectively (Figure S2C of the Supporting Information).

5HPP-33 Suppressed the Dynamic Instability of Microtubules in Live MCF-7 Cells. EGFP-tubulin-expressing MCF-7 cells were incubated either with the vehicle or with 5 and 10 μM 5HPP-33 for 3 h. The dynamics of individual interphase microtubules in live MCF-7 cells were monitored by time-lapse imaging.[47] The life history traces of individual microtubules with respect to time were plotted, and various parameters of dynamic instability were estimated from the plots. As reported previously,[32,33,47] microtubules in the vehicle-treated (control) cells displayed stochastic transitions among the growth, shortening, and pause states (Figure 3). However, 5HPP-33 treatment reduced the dynamic instability of microtubules (Figure 3 and Table 1). The growth rate of microtubules was reduced by 34 and 36% in the presence of 5 and 10 μM 5HPP-33, respectively. The compound also inhibited the length of growing excursion and the percentage of time microtubules spent in the growing phase. In addition, 5HPP-33 reduced the rate and extent of the shortening excursions of microtubules. The catastrophe frequency per minute was decreased by 32 and 51% in the presence of 5 and 10 μM 5HPP-33, respectively. However, the compound did not significantly influence the time-based rescue frequency. Interestingly, 5HPP-33 significantly increased both length-based rescue and catastrophe frequencies, suggesting that it suppressed growing and shortening length excursions. 5HPP-33 strongly increased the time the microtubule spent in the pause state. The dynamicity (dimer exchange per unit time) of microtubules was reduced by 62 and 70% in the presence of 5 and 10 μM 5HPP-33, respectively.

Table 1. Effects of 5HPP-33 on Various Parameters of the Dynamic Instability of Microtubules[a]

	control	5 μM 5HPP-33	10 μM 5HPP-33
growth rate (μm/min)	17 ± 5.5	11.3 ± 2.7[b]	10.9 ± 2[b]
shortening rate (μm/min)	17.5 ± 4.8	11.7 ± 1.9[b]	11.5 ± 2.5[b]
growth length (μm)	1.7 ± 0.8	0.8 ± 0.2[c]	0.77 ± 0.2[c]
shortening length (μm)	1.5 ± 0.6	1.0 ± 0.2[c]	0.9 ± 0.4[b]
growth time (min)	0.98 ± 0.26	0.40 ± 15[c]	0.37 ± 17[c]
shortening time (min)	0.75 ± 0.18	0.56 ± 0.18[b]	0.37 ± 0.18[b]
pause time (min)	0.84 ± 0.31	1.60 ± 0.28[b]	1.75 ± 0.35[b]
% time spent in growth	38.2 ± 9.50	15.3 ± 5.7[c]	15.1 ± 7[c]
% time spent in shortening	29.2 ± 7.1	21.9 ± 7[b]	14.9 ± 7.4[c]
% time spent in pause	32.6 ± 12	62.5 ± 11.4[c]	69.9 ± 12.7[c]
rescue frequency (no. of events/min)	11.4 ± 2	12.0 ± 2.5[d]	12.8 ± 3.0[d]
catastrophe frequency (no. of events/min)	4.7 ± 1.2	3.2 ± 1[b]	2.3 ± 1.3[d]
rescue frequency (no. of events/μm)	0.7 ± 0.24	1 ± 0.27[b]	1.2 ± 0.45[d]
catastrophe frequency (no. of events/μm)	0.5 ± 0.2	1.6 ± 0.7[c]	1.3 ± 0.9[d]
dynamicity (μm/min)	11.9 ± 4.6	4.5 ± 2[c]	3.6 ± 2.1[c]

[a]Data are average ± the standard deviation. n = 25 microtubules in each case. The significance test was done by one-way ANOVA. [b]P < 0.05. [c]P < 0.001. [d]Not significant.

5HPP-33 Inhibited MAP-Rich Tubulin Assembly. Consistent with the previous studies,[22,23,48] 5HPP-33 was found to inhibit the assembly of MAP-rich tubulin in a concentration-dependent manner (Figure S3A of the Supporting Information). For example, 14 ± 4, 23 ± 4, 37 ± 9, and 63 ± 17% decreases in the level of assembly of microtubules occurred in the presence of 2.5, 5, 10, and 20 μM 5HPP-33, respectively. 5HPP-33 also increased the lag time for MAP-rich tubulin assembly, indicating that it inhibited the nucleation of microtubules. In addition, 5HPP-33 inhibited the assembly of phosphocellulose-purified tubulin in the presence of 1 M glutamate (Figure S3B of the Supporting Information). For example, 5, 10, 20, and 30 μM 5HPP-33 inhibited the extent of the tubulin assembly by 11 ± 6, 39 ± 8, 53 ± 27, and 59 ± 28%, respectively. 5HPP-33 also inhibited DMSO-induced assembly of purified tubulin in a concentration-dependent manner (Figure S3C of the Supporting Information). For example, 15 ± 6, 31 ± 9, and 42 ± 16% inhibition of tubulin assembly occurred in the presence of 10, 20, and 30 μM 5HPP-33, respectively. Further, electron microscopic analysis suggested that 5HPP-33 inhibited the assembly of both MAP-rich tubulin and tubulin (Figure S4 of the Supporting Information).

5HPP-33 Bound to Purified Tubulin with a Weak Affinity. 5HPP-33 reduced the intrinsic fluorescence of tubulin in a concentration-dependent manner (Figure 4AI). The dissociation constant (K_d) for binding of 5HPP-33 to tubulin was determined to be 45 ± 12 μM from the fluorescence quenching data (Figure 4AII). 5HPP-33 displayed weak fluorescence. The fluorescence intensity of 5HPP-33 increased upon incubation with tubulin, suggesting that it binds to tubulin (Figure 4BI). A K_d for binding of 5HPP-33 to tubulin was determined to be 78 ± 18 μM from the dose-dependent increase in the fluorescence of 5HPP-33 in the presence of tubulin (Figure 4BII).

Determination of the Binding Site of 5HPP-33 on Tubulin. The binding of 5HPP-33 with tubulin increased the fluorescence of 5HPP-33 (Figure 4BI). The preincubation of vinblastine with tubulin reduced the extent of development of the fluorescence of 5HPP-33, indicating that vinblastine inhibited the binding of 5HPP-33 to tubulin (Figure 4CI,II). In a separate experiment, BODIPY FL-vinblastine, a fluorescent analogue of vinblastine was used to examine the effect of 5HPP-33 on the binding of vinblastine to tubulin.[31] 5HPP-33 reduced the development of the fluorescence of BODIPY FL-vinblastine, suggesting that 5HPP-33 shares its binding site on tubulin with vinblastine (Figure 4DI,II). Podophyllotoxin did not inhibit the development of 5HPP-33 fluorescence in the presence of tubulin, indicating that 5HPP-33 does not share its binding site on tubulin with podophyllotoxin (Figure 4E).

Computational Analysis of Binding of 5HPP-33 to Tubulin. To gain further insight into the binding interaction of 5HPP-33 and tubulin, we performed molecular docking studies of 5HPP-33 and vinblastine binding on tubulin. The binding energy for control docking of vinblastine on the tubulin dimer was −11.72 kcal/mol for the minimum energy docked conformation. A comparison between the X-ray crystallo-

DOI: 10.1021/bi501429j
Biochemistry 2015, 54, 2149−2159

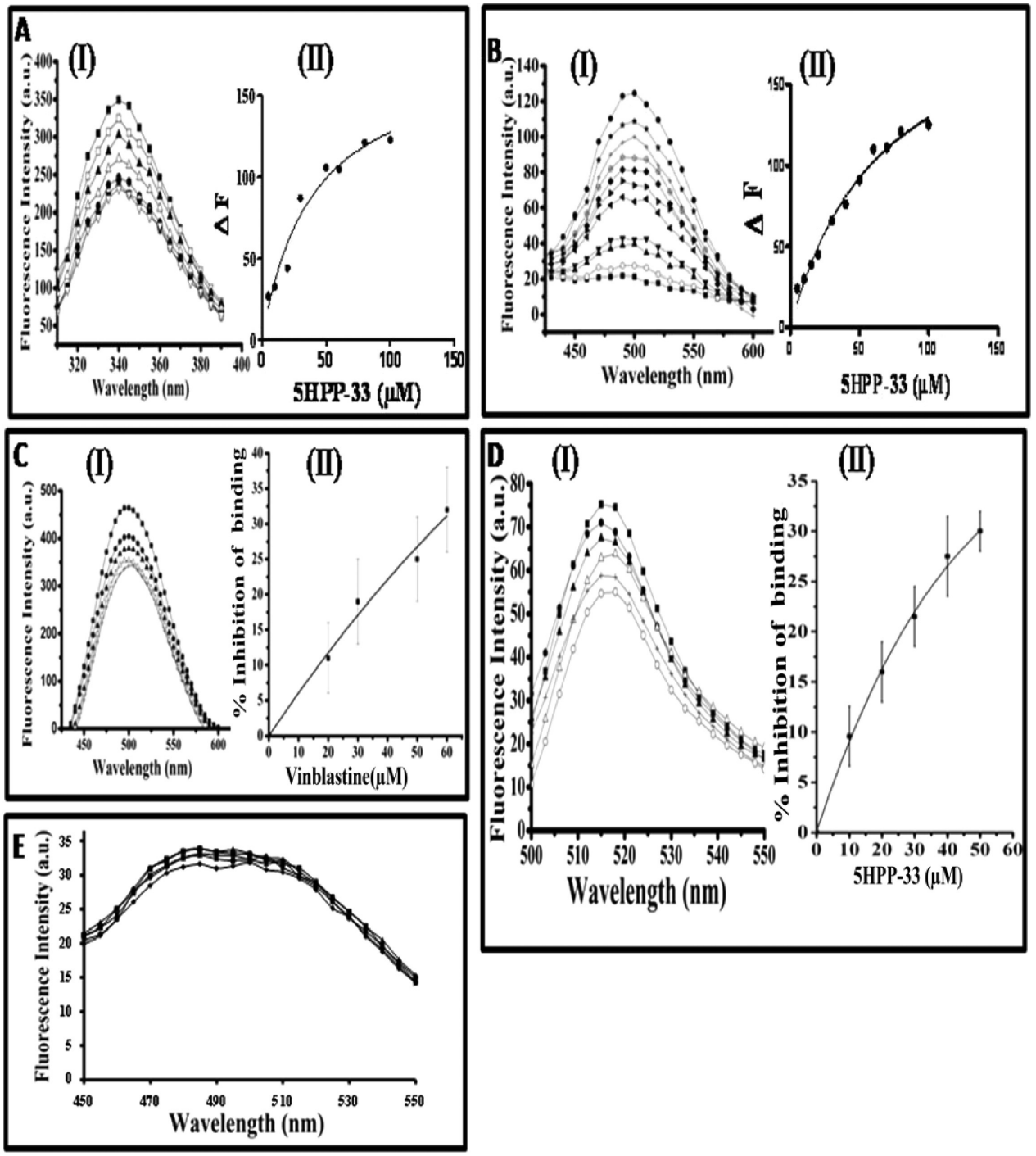

Figure 4. 5HPP-33 bound to tubulin. Tubulin (2 μM) was incubated in the absence (■) and presence of 10 (□), 20 (▲), 30 (△), 50 (●), 60 (○), 80 (▼) and 100 μM 5HPP-33 (▽) for 20 min at 25 °C. (A) 5HPP-33 reduced the intrinsic tryptophan fluorescence of tubulin in a concentration-dependent manner (I). The decrease in the fluorescence intensity of tubulin was fit in a binding isotherm (II). (B) The fluorescence intensity of 5HPP-33 increased upon binding to tubulin. The spectrum of 5HPP-33 was subtracted from the spectrum of 5HPP-33 in the presence of tubulin. Shown are the subtracted spectra of different concentrations of 5HPP-33 [5 (■), 10 (○), 15 (▲), 20 (▼), 30 (left-pointing triangle), 40 (right-pointing triangle), 50 (◆), 60 (⊕), 70 (+), 80 (★), and 100 μM (●)] (I). The increase in the fluorescence intensity of 5HPP-33 upon binding to tubulin was plotted against 5HPP-33 concentration to obtain K_d (II). (C) Tubulin (3 μM) was incubated without 0 (■) or with 20 (●), 30 (▲), 50 (△), and 60 μM vinblastine (+) for 30 min at 25 °C. Subsequently, the reaction mixtures were incubated with 10 μM 5HPP-33 for 10 min at 25 °C. The fluorescence spectra were noted (I), and the percent inhibition of 5HPP-33 binding was calculated (II). (D) Tubulin (2 μM) was incubated without or with different concentrations of 5HPP-33 for 30 min at 25 °C. Then, the mixtures were incubated with 2 μM BODIPY FL-vinblastine for 20 min at 25 °C. Effects of different concentrations of 5HPP-33 [0 (■), 10 (●), 20 (▲), 30 (△), 40 (+), and 50 μM (○)] on the development of the fluorescence of BODIPY FL-vinblastine upon tubulin binding are shown (I), and the percent inhibition of the binding of BODIPY FL-vinblastine was calculated (II). (E) Tubulin (3 μM) was incubated without (◆) or with different concentrations [10 (■), 20 (▲), 30 (●), and 50 μM (−)] of podophyllotoxin for 30 min at 25 °C. Then, 5HPP-33 (10 μM) was added to the reaction mixtures, and they were incubated for an additional 20 min at 25 °C. The fluorescence spectra were recorded using 350 nm as the excitation wavelength.

DOI: 10.1021/bi501429j
Biochemistry 2015, 54, 2149−2159

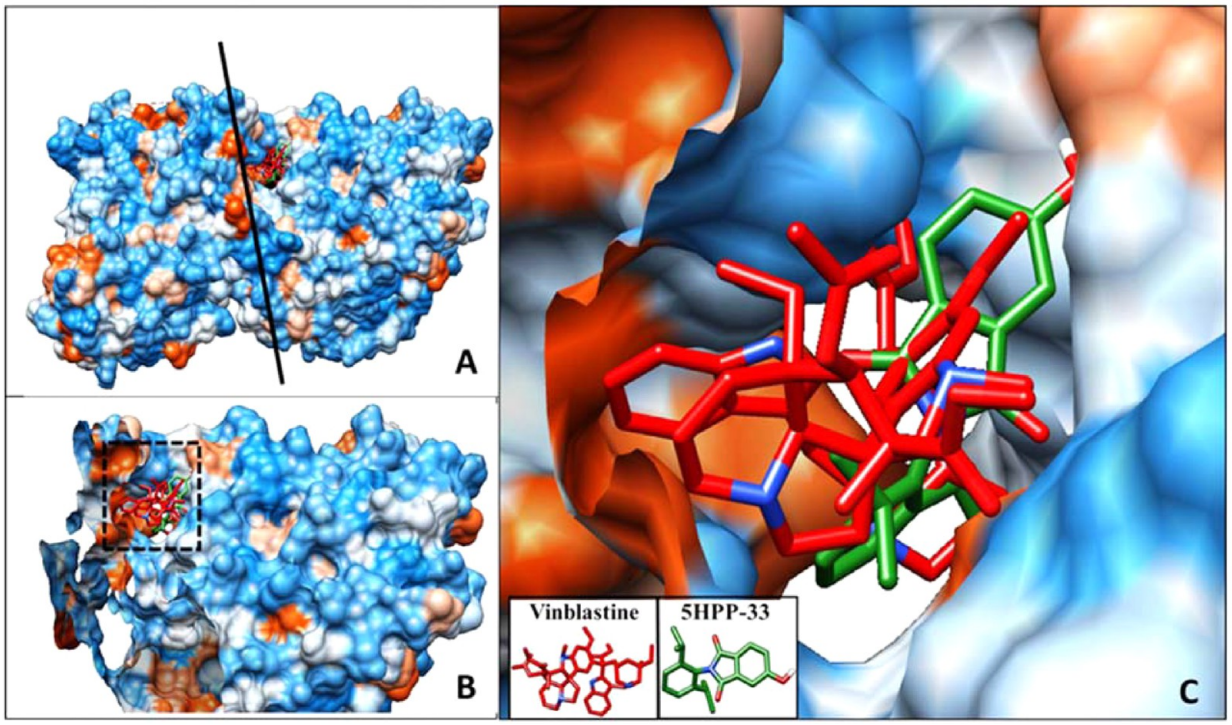

Figure 5. Docking of 5HPP-33 to the tubulin dimer. Hydrophobic surface of chains B (β) and C (α) of PDB entry 1Z2B. The hydrophobic surface is shown in dodger blue for the most hydrophilic, white for neutral, and orange-red for the most hydrophobic surface. 5HPP-33 is colored forest green, while vinblastine is colored red. Red, blue, and white sticks represent oxygen, nitrogen, and hydrogen atoms, respectively, of the ligands, 5HPP-33, and vinblastine. (A) The oblique line shows the axis where the $\beta-\alpha$ interface of PDB entry 1Z2B is cut to show the cross-sectional view of the binding pockets of both 5HPP-33 and vinblastine in panel B. (B) Cross-sectional view of 5HPP-33 and the vinblastine binding pocket over the hydrophobic surface. (C) The dotted square box shown in panel B is enlarged to give a close-up view of the 5HPP-33 and vinblastine binding pockets. Vinblastine (red) and 5HPP-33 (forest green) are shown as insets in panel C. An overlap of the binding pockets of vinblastine and 5HPP-33 can be clearly seen in panel C.

graphically determined structure and the docked conformation was made. The rmsd between the "predicted" and crystallographically determined binding modes of vinblastine was found to be 0.818 Å, which because it was <2 Å indicated that the docking methodology used was appropriate.[40]

Then, docking of 5HPP-33 was performed with tubulin by adopting the exact procedure as employed for vinblastine (control). The analysis suggested that the 5HPP-33 binding site is at the $\beta-\alpha$ tubulin interface (Figure 5A,B). The estimated binding energy of this pose was found to be −6.86 kcal/mol. The interaction of 5HPP-33 with the tubulin dimer revealed that 5HPP-33 was forming contacts with residues Lys326 and Asn329 of chain C and Pro175, Lys176, Val177, Ser178, Asp179, Tyr210, Phe214, Leu219, Thr220, and Pro222 of chain B. Thus, we concluded that the 5HPP-33 binding pocket consists of amphipathic amino acids (both hydrophobic and hydrophilic residues). Moreover, 5HPP-33 can make two hydrogen bonds in the docked conformation, one each with Asn329 and Thr220. More importantly, the binding pockets of 5HPP-33 and vinblastine were found to partially overlap (Figure 5C)

DISCUSSION

In this study, 5HPP-33 was found to bind to pure tubulin with a weak affinity at the vinblastine site and to inhibit microtubule assembly *in vitro* and in cultured MCF-7 cells. 5HPP-33 dampened the dynamics of individual microtubules in live MCF-7 cells and caused mitotic arrest and multipolar spindle formation in MCF-7 cells.

5HPP-33 Shares a Vinblastine Binding Site on Tubulin. The binding affinities of 5HPP-33 with tubulin were determined to be 45 ± 12 and 78 ± 18 μM by using the quenching of the tryptophan fluorescence of tubulin and the enhancement of 5HPP-33 fluorescence upon binding to tubulin, respectively. The K_d estimated by the two methods differed by ∼1.8-fold, which could be attributed to the difference in the two fluorescence techniques. Earlier, the K_d of the vinblastine−tubulin interaction was reported to vary from 0.54 to 43 μM,[49,50] indicating that the estimated dissociation constant depends on the techniques used, solution conditions, and protein preparations. Similar results were also obtained for other inhibitors of tubulin. Nonetheless, the data obtained in this study indicated that 5HPP-33 binds to tubulin with a weak affinity.

A competition assay involving 5HPP-33 and vinblastine indicated that vinblastine partially inhibited the binding of 5HPP-33 to tubulin. In a complementary assay, 5HPP-33 was found to partially inhibit the binding of BODIPY FL-vinblastine to tubulin. The results together indicated that 5HPP-33 and vinblastine share their binding sites on tubulin. Further, a molecular docking analysis suggested that 5HPP-33 binds to tubulin at the vinblastine site. Using radioactive vinblastine, it was reported that 5HPP-33 did not inhibit the binding of vinblastine to tubulin.[23] Vinblastine was found to bind to tubulin with a K_d of 0.31 ± 0.03 μM using intrinsic tryptophyan fluorescence quenching,[51] indicating that vinblastine binds to tubulin with an affinity much higher than that of 5HPP-33. Therefore, it was likely that 5HPP-33 could not inhibit the

DOI: 10.1021/bi501429j
Biochemistry 2015, 54, 2149−2159

binding of radioactive vinblastine to tubulin. Because vinblastine binds to tubulin with an affinity higher than that of 5HPP-33, it could inhibit the binding of 5HPP-33 to tubulin. In BODIPY FL-vinblastine, a bulky molecule (4,4-difluoro-5,7-dimethyl-4-bora-3a,4a-diaza-*s*-indacene) is covalently attached to vinblastine.[52] Thus, BODIPY FL-vinblastine may bind to tubulin weakly as compared to vinblastine. Therefore, 5HPP-33 may inhibit the binding of BODIPY FL-vinblastine to tubulin.

Effects of 5HPP-33 on Microtubule Dynamics and Mechanism of Inhibition of Cell Proliferation. 5HPP-33 reduced the rate and extents of growing and shortening phases of microtubules. It increased the time microtubules spent in the pause state and strongly dampened the microtubule dynamics. Similar to other microtubule-targeting agents, the suppression of microtubule dynamics by 5HPP-33 can occur via its binding to the plus ends of microtubules, thus hampering the dynamics of tubulin addition or removal at the tip of the microtubules. In 5HPP-33-treated cells, kinetically suppressed microtubules may not be able to make proper attachment with the kinetochores. The altered attachments of microtubules to kinetochores may activate the spindle check point proteins leading to the mitotic block. The mitotic spindles formed in the presence of 5HPP-33 were aberrant with an increase in the number of monopolar and multipolar cells. The distance between two poles of a bipolar mitotic spindle was also reduced, which may be due to the suppression of microtubule dynamics, thus affecting force generation for centrosome separation. The number of multinucleated interphase-like cells increased after treatment for 48 h with 5HPP-33. The formation of multinucleated cells in the presence of 5HPP-33 after treatment for 48 h suggested that the multipolar mitotic cells continued to progress through the cell cycle probably because of the lack of a stringent cell cycle control mechanism in these cells.[32]

A Possible Mechanism for Thalidomide-Mediated Teratogenicity. During cell migration, asymmetrical regulation of microtubule dynamics and stability at the front and rear sides of a migrating cell gives rise to the polarity of the microtubule network, which in turn helps in the migration of cells.[26,53] Microtubule dynamics plays crucial roles in angiogenesis and cell migration;[26,54] therefore, thalidomide-mediated anti-angiogenic effects can be due to its metabolites having inhibitory effects on microtubule dynamics. This notion is supported by the fact that the perturbation of microtubule assembly in sea urchin embryo causes teratogenicity.[55] The exposure of hamster embryo to vinblastine and vincristine caused congenital malformation.[56] Colchicine also passes through the placental barrier and is shown to be teratogenic in animals.[57] It is reported that microtubule acetylation in the direction of cell migration is associated with the establishment of the polarized cell morphology.[26] 5HPP-33 increased the level of global acetylation of microtubules (Figure S2A of the Supporting Information), which might render a cell non-responsive to migrational cues.[26] Suppression of microtubule dynamics also leads to nuclear accumulation of p53.[58] p53 is suggested to play an important role in the apoptosis and induction of birth defects by teratogens.[59−61] p53 is known to suppress vascular endothelial growth factor (VEGF)[62,63] by forming transcriptional repression complex,[64] and thus, it can suppress angiogenesis in the developing embryo.[65]

■ ASSOCIATED CONTENT

Supporting Information

5HPP-33 treatment that depolymerized microtubules in MDA-MB231 (Figure S1), effects of 5HPP-33 on microtubule acetylation in MCF-7 cells (Figure S2A), MCF-7 cells treated with 5HPP-33 that caused mitotic block (Figure S2B), MCF-7 cells treated with 10 and 20 μM 5HPP-33 for 48 h that displayed multinucleation (Figure S2C), 5HPP-33 that inhibited the assembly of MAP-rich tubulin (Figure S3A), 5HPP-33 that inhibited the assembly of purified tubulin in the presence of 1 M glutamate (Figure S3B) and also inhibited DMSO-induced assembly of purified tubulin (Figure S3C) *in vitro*, and the inhibitory effects of 5HPP-33 on the assembly of MAP-rich tubulin and pure tubulin also analyzed by electron microscopy (Figure S4). This material is available free of charge via the Internet at http://pubs.acs.org.

■ AUTHOR INFORMATION

Corresponding Author

*Department of Biosciences and Bioengineering, Indian Institute of Technology Bombay, Mumbai 400076, India. Telephone: +91-22-25767838. Fax: +91-22-25723480. E-mail: panda@iitb.ac.in.

Funding

This work was supported by a grant from the Department of Biotechnology, Government of India, to D.P. A. Kunwar is partly supported by the Industrial Research and Consultancy Centre at IIT Bombay and partly by an Innovative Young Biotechnologist Award from DBT (Grant BT/06/IYBA/2012). A.R. thanks the University Grants Commission for a research fellowship.

Notes

The authors declare no competing financial interest.

■ ACKNOWLEDGMENTS

We thank the Centre for Research in Nanotechnology and Science, Indian Institute of Technology Bombay, for use of the confocal microscopy facility. This paper is dedicated to Dr. I Ojima on his 70th birthday.

■ ABBREVIATIONS

5HPP-33, 5-hydroxy-2-(2,6-diisopropylphenyl)-1*H*-isoindole-1,3-dione; IC_{50}, half-maximal inhibitory concentration; MEM, minimal essential medium; VEGF, vascular endothelial growth factor; EGFP-tubulin, enhanced green fluorescent protein-bound tubulin; K_d, dissociation constant; MAP, microtubule-associated protein.

■ REFERENCES

(1) Hashimoto, Y. (2008) Thalidomide as a multi-template for development of biologically active compounds. *Arch. Pharm. (Weinheim, Ger.) 341*, 536−547.

(2) Ito, T., Ando, H., and Handa, H. (2011) Teratogenic effects of thalidomide: Molecular mechanisms. *Cell. Mol. Life Sci. 68*, 1569−1579.

(3) Knobloch, J., Schmitz, I., Gotz, K., Schulze-Osthoff, K., and Ruther, U. (2008) Thalidomide induces limb anomalies by PTEN stabilization, Akt suppression, and stimulation of caspase-dependent cell death. *Mol. Cell. Biol. 28*, 529−538.

(4) Nishimura, K., Hashimoto, Y., and Iwasaki, S. (1994) Enhancement of phorbol ester-induced production of tumor necrosis factor α by thalidomide. *Biochem. Biophys. Res. Commun. 199*, 455−460.

DOI: 10.1021/bi501429j
Biochemistry 2015, 54, 2149−2159

(5) Kita, T., Takahashi, H., and Hashimoto, Y. (2001) Thymidine phosphorylase inhibitors with a homophthalimide skeleton. *Biol. Pharm. Bull. 24*, 860−862.
(6) Sano, H., Noguchi, T., Tanatani, A., Miyachi, H., and Hashimoto, Y. (2004) N-Phenylphthalimide-type cyclooxygenase (COX) inhibitors derived from thalidomide: Substituent effects on subtype selectivity. *Chem. Pharm. Bull. 52*, 1021−1022.
(7) Shinji, C., Maeda, S., Imai, K., Yoshida, M., Hashimoto, Y., and Miyachi, H. (2006) Design, synthesis, and evaluation of cyclic amide/imide-bearing hydroxamic acid derivatives as class-selective histone deacetylase (HDAC) inhibitors. *Bioorg. Med. Chem. 14*, 7625−7651.
(8) Noguchi, T., Fujimoto, H., Sano, H., Miyajima, A., Miyachi, H., and Hashimoto, Y. (2005) Angiogenesis inhibitors derived from thalidomide. *Bioorg. Med. Chem. Lett. 15*, 5509−5513.
(9) Noguchi, T., Miyachi, H., Katayama, R., Naito, M., and Hashimoto, Y. (2005) Cell differentiation inducers derived from thalidomide. *Bioorg. Med. Chem. Lett. 15*, 3212−3215.
(10) Inatsuki, S., Noguchi, T., Miyachi, H., Oda, S., Iguchi, T., Kizaki, M., Hashimoto, Y., and Kobayashi, H. (2005) Tubulin-polymerization inhibitors derived from thalidomide. *Bioorg. Med. Chem. Lett. 15*, 321−325.
(11) Yanagawa, T., Noguchi, T., Miyachi, H., Kobayashi, H., and Hashimoto, Y. (2006) Tubulin polymerization inhibitors with a fluorinated phthalimide skeleton derived from thalidomide. *Bioorg. Med. Chem. Lett. 16*, 4748−4751.
(12) Vargesson, N. (2013) Thalidomide Embryopathy: An Enigmatic Challenge. *ISRN Developmental Biology 2013*, 18.
(13) Knobloch, J., Reimann, K., Klotz, L. O., and Ruther, U. (2008) Thalidomide resistance is based on the capacity of the glutathione-dependent antioxidant defense. *Mol. Pharmaceutics 5*, 1138−1144.
(14) Lu, J., Helsby, N., Palmer, B. D., Tingle, M., Baguley, B. C., Kestell, P., and Ching, L. M. (2004) Metabolism of thalidomide in liver microsomes of mice, rabbits, and humans. *J. Pharmacol. Exp. Ther. 310*, 571−577.
(15) Ito, T., and Handa, H. (2012) Deciphering the mystery of thalidomide teratogenicity. *Congenital Anomalies 52*, 1−7.
(16) Stephens, T. D. (1988) Proposed mechanisms of action in thalidomide embryopathy. *Teratology 38*, 229−239.
(17) Parman, T., Wiley, M. J., and Wells, P. G. (1999) Free radical-mediated oxidative DNA damage in the mechanism of thalidomide teratogenicity. *Nat. Med. 5*, 582−585.
(18) D'Amato, R. J., Loughnan, M. S., Flynn, E., and Folkman, J. (1994) Thalidomide is an inhibitor of angiogenesis. *Proc. Natl. Acad. Sci. U.S.A. 91*, 4082−4085.
(19) Mabjeesh, N. J., Escuin, D., LaVallee, T. M., Pribluda, V. S., Swartz, G. M., Johnson, M. S., Willard, M. T., Zhong, H., Simons, J. W., and Giannakakou, P. (2003) 2ME2 inhibits tumor growth and angiogenesis by disrupting microtubules and dysregulating HIF. *Cancer Cell 3*, 363−375.
(20) Jordan, M. A., and Wilson, L. (2004) Microtubules as a target for anticancer drugs. *Nat. Rev. Cancer 4*, 253−265.
(21) Yvon, A. M., Wadsworth, P., and Jordan, M. A. (1999) Taxol suppresses dynamics of individual microtubules in living human tumor cells. *Mol. Biol. Cell 10*, 947−959.
(22) Inatsuki, S., Noguchi, T., Miyachi, H., Oda, S., Iguchi, T., Kizaki, M., Hashimoto, Y., and Kobayashi, H. (2005) Tubulin-polymerization inhibitors derived from thalidomide. *Bioorg. Med. Chem. Lett. 15*, 321−325.
(23) Aoyama, H., Noguchi, T., Misawa, T., Nakamura, T., Miyachi, H., Hashimoto, Y., and Kobayashi, H. (2007) Development of tubulin-polymerization inhibitors based on the thalidomide skeleton. *Chem. Pharm. Bull. 55*, 944−949.
(24) Iguchi, T., Oda-Nakazato, S., Noguchi, T., Hashimoto, Y., Hattori, Y., Yamada, T., Ikeda, Y., and Kizaki, M. (2008) 5HPP-33, a Novel Tubulin-Polymerization Inhibitor Derived from Thalidomide, Directly Inhibits Proliferation and Induces Apoptosis of Human Multiple Myeloma Cells. *Int. J. Mol. Med. 21*, 163−168.
(25) Li, P. K., Pandit, B., Sackett, D. L., Hu, Z., Zink, J., Zhi, J., Freeman, D., Robey, R. W., Werbovetz, K., Lewis, A., and Li, C. (2006) A thalidomide analogue with in vitro antiproliferative, antimitotic, and microtubule-stabilizing activities. *Mol. Cancer Ther. 5*, 450−456.
(26) Kapoor, S., and Panda, D. (2012) Kinetic stabilization of microtubule dynamics by indanocine perturbs EB1 localization, induces defects in cell polarity and inhibits migration of MDA-MB-231 cells. *Biochem. Pharmacol. 83*, 1495−1506.
(27) Tseng, C. M., Hsiao, Y. H., Su, V. Y., Su, K. C., Wu, Y. C., Chang, K. T., and Perng, D. W. (2013) The suppression effects of thalidomide on human lung fibroblasts: Cell proliferation, vascular endothelial growth factor release, and collagen production. *Lung 191*, 361−368.
(28) Kurosaka, S., and Kashina, A. (2008) Cell biology of embryonic migration. *Birth Defects Res., Part C 84*, 102−122.
(29) Skehan, P., Storeng, R., Scudiero, D., Monks, A., McMahon, J., Vistica, D., Warren, J. T., Bokesch, H., Kenney, S., and Boyd, M. R. (1990) New colorimetric cytotoxicity assay for anticancer-drug screening. *J. Natl. Cancer Inst. 82*, 1107−1112.
(30) Gireesh, K. K., Rashid, A., Chakraborti, S., Panda, D., and Manna, T. (2012) CIL-102 binds to tubulin at colchicine binding site and triggers apoptosis in MCF-7 cells by inducing monopolar and multinucleated cells. *Biochem. Pharmacol. 84*, 633−645.
(31) Rai, A., Surolia, A., and Panda, D. (2012) An antitubulin agent BCFMT inhibits proliferation of cancer cells and induces cell death by inhibiting microtubule dynamics. *PLoS One 7*, e44311.
(32) Mohan, R., and Panda, D. (2008) Kinetic stabilization of microtubule dynamics by estramustine is associated with tubulin acetylation, spindle abnormalities, and mitotic arrest. *Cancer Res. 68*, 6181−6189.
(33) Rathinasamy, K., and Panda, D. (2008) Kinetic stabilization of microtubule dynamic instability by benomyl increases the nuclear transport of p53. *Biochem. Pharmacol. 76*, 1669−1680.
(34) Walker, R. A., O'Brien, E. T., Pryer, N. K., Soboeiro, M. F., Voter, W. A., Erickson, H. P., and Salmon, E. D. (1988) Dynamic instability of individual microtubules analyzed by video light microscopy: Rate constants and transition frequencies. *J. Cell Biol. 107*, 1437−1448.
(35) Hamel, E., and Lin, C. M. (1981) Glutamate-induced polymerization of tubulin: Characteristics of the reaction and application to the large-scale purification of tubulin. *Arch. Biochem. Biophys. 209*, 29−40.
(36) Chatterji, B. P., Banerjee, M., Singh, P., and Panda, D. (2010) HMBA depolymerizes microtubules, activates mitotic checkpoints and induces mitotic block in MCF-7 cells by binding at the colchicine site in tubulin. *Biochem. Pharmacol. 80*, 50−61.
(37) Bradford, M. M. (1976) A rapid and sensitive method for the quantitation of microgram quantities of protein utilizing the principle of protein-dye binding. *Anal. Biochem. 72*, 248−254.
(38) Shelanski, M. L., Gaskin, F., and Cantor, C. R. (1973) Microtubule assembly in the absence of added nucleotides. *Proc. Natl. Acad. Sci. U.S.A. 70*, 765−768.
(39) Bhattacharyya, B., Kapoor, S., and Panda, D. (2010) Fluorescence spectroscopic methods to analyze drug-tubulin interactions. *Methods Cell Biol. 95*, 301−329.
(40) Morris, G. M., Huey, R., Lindstrom, W., Sanner, M. F., Belew, R. K., Goodsell, D. S., and Olson, A. J. (2009) AutoDock4 and AutoDockTools4: Automated docking with selective receptor flexibility. *J. Comput. Chem. 30*, 2785−2791.
(41) Schuttelkopf, A. W., and van Aalten, D. M. (2004) PRODRG: A tool for high-throughput crystallography of protein-ligand complexes. *Acta Crystallogr. D60*, 1355−1363.
(42) Venghateri, J. B., Gupta, T. K., Verma, P. J., Kunwar, A., and Panda, D. (2013) Ansamitocin P3 depolymerizes microtubules and induces apoptosis by binding to tubulin at the vinblastine site. *PLoS One 8* (10), e75182.
(43) Hetenyi, C., and van der Spoel, D. (2002) Efficient docking of peptides to proteins without prior knowledge of the binding site. *Protein Sci. 11*, 1729−1737.

DOI: 10.1021/bi501429j
Biochemistry 2015, 54, 2149−2159

(44) Pettersen, E. F., Goddard, T. D., Huang, C. C., Couch, G. S., Greenblatt, D. M., Meng, E. C., and Ferrin, T. E. (2004) UCSF Chimera: A visualization system for exploratory research and analysis. *J. Comput. Chem. 25*, 1605−1612.
(45) Rai, A., Gupta, T. K., Kini, S., Kunwar, A., Surolia, A., and Panda, D. (2013) CXI-benzo-84 reversibly binds to tubulin at colchicine site and induces apoptosis in cancer cells. *Biochem. Pharmacol. 86*, 378−391.
(46) Goto, H., Tomono, Y., Ajiro, K., Kosako, H., Fujita, M., Sakurai, M., Okawa, K., Iwamatsu, A., Okigaki, T., Takahashi, T., and Inagaki, M. (1999) Identification of a novel phosphorylation site on histone H3 coupled with mitotic chromosome condensation. *J. Biol. Chem. 274*, 25543−25549.
(47) Dhamodharan, R., Jordan, M. A., Thrower, D., Wilson, L., and Wadsworth, P. (1995) Vinblastine suppresses dynamics of individual microtubules in living interphase cells. *Mol. Biol. Cell 6*, 1215−1229.
(48) Kizaki, M., and Hashimoto, Y. (2008) New tubulin polymerization inhibitor derived from thalidomide: Implications for anti-myeloma therapy. *Curr. Med. Chem. 15*, 754−765.
(49) Safa, A. R., Hamel, E., and Felsted, R. L. (1987) Photoaffinity labeling of tubulin subunits with a photoactive analogue of vinblastine. *Biochemistry 26*, 97−102.
(50) Lee, J. C., Harrison, D., and Timasheff, S. N. (1975) Interaction of Vinblastine with Calf Brain Microtubule Protein. *J. Biol. Chem. 250*, 9276−9282.
(51) Cormier, A., Knossow, M., Wang, C., and Gigant, B. (2010) The binding of vinca domain agents to tubulin: Structural and biochemical studies. *Methods Cell Biol. 95*, 373−390.
(52) Lin, W., and Chen, T. (2013) A vinblastine fluorescent probe for pregnane X receptor in a time-resolved fluorescence resonance energy transfer assay. *Anal. Biochem. 443*, 252−260.
(53) Etienne-Manneville, S. (2013) Microtubules in cell migration. *Annu. Rev. Cell Dev. Biol. 29*, 471−499.
(54) Bijman, M. N., van Nieuw Amerongen, G. P., Laurens, N., van Hinsbergh, V. W., and Boven, E. (2006) Microtubule-targeting agents inhibit angiogenesis at subtoxic concentrations, a process associated with inhibition of Rac1 and Cdc42 activity and changes in the endothelial cytoskeleton. *Mol. Cancer Ther. 5*, 2348−2357.
(55) Estus, S., and Blumer, J. L. (1989) Role of microtubule assembly in phenytoin teratogenic action in the sea urchin (*Arbacia punctulata*) embryo. *Mol. Pharmacol. 36*, 708−715.
(56) Ferm, V. H. (1963) Congenital malformations in hamster embryos after treatment with vinblastine and vincristine. *Science 141*, 426.
(57) Levy, M., Spino, M., and Read, S. E. (1991) Colchicine: A state-of-the-art review. *Pharmacotherapy 11*, 196−211.
(58) Giannakakou, P., Nakano, M., Nicolaou, K. C., O'Brate, A., Yu, J., Blagosklonny, M. V., Greber, U. F., and Fojo, T. (2002) Enhanced microtubule-dependent trafficking and p53 nuclear accumulation by suppression of microtubule dynamics. *Proc. Natl. Acad. Sci. U.S.A. 99*, 10855−10860.
(59) Hosako, H., Little, S. A., Barrier, M., and Mirkes, P. E. (2007) Teratogen-induced activation of p53 in early postimplantation mouse embryos. *Toxicol. Sci. 95*, 257−269.
(60) Wubah, J. A., Ibrahim, M. M., Gao, X., Nguyen, D., Pisano, M. M., and Knudsen, T. B. (1996) Teratogen-induced eye defects mediated by p53-dependent apoptosis. *Curr. Biol. 6*, 60−69.
(61) Pekar, O., Molotski, N., Savion, S., Fein, A., Toder, V., and Torchinsky, A. (2007) p53 regulates cyclophosphamide teratogenesis by controlling caspases 3, 8, 9 activation and NF-κB DNA binding. *Reproduction 134*, 379−388.
(62) Farhang Ghahremani, M., Goossens, S., and Haigh, J. J. (2013) p53 family and VEGF regulation: "It's complicated". *Cell Cycle 12*, 1331−1332.
(63) Farhang Ghahremani, M., Goossens, S., Nittner, D., Bisteau, X., Bartunkova, S., Zwolinska, A., Hulpiau, P., Haigh, K., Haenebalcke, L., Drogat, B., Jochemsen, A., Roger, P. P., Marine, J. C., and Haigh, J. J. (2013) p53 promotes VEGF expression and angiogenesis in the absence of an intact p21-Rb pathway. *Cell Death Differ. 20*, 888−897.
(64) Qin, G., Kishore, R., Dolan, C. M., Silver, M., Wecker, A., Luedemann, C. N., Thorne, T., Hanley, A., Curry, C., Heyd, L., Dinesh, D., Kearney, M., Martelli, F., Murayama, T., Goukassian, D. A., Zhu, Y., and Losordo, D. W. (2006) Cell cycle regulator E2F1 modulates angiogenesis via p53-dependent transcriptional control of VEGF. *Proc. Natl. Acad. Sci. U.S.A. 103*, 11015−11020.
(65) Breier, G., Albrecht, U., Sterrer, S., and Risau, W. (1992) Expression of vascular endothelial growth factor during embryonic angiogenesis and endothelial cell differentiation. *Development 114*, 521−532.

DOI: 10.1021/bi501429j
Biochemistry 2015, 54, 2149−2159